J Mater Sci (2020) 55:3926–3939

Electronic materials

PVDF–ferrite composites with dual magneto-piezoelectric response for flexible electronics applications: synthesis and functional properties

Felicia Gheorghiu[1,*], Roxana Stanculescu[2], Lavinia Curecheriu[3], Elisabetta Brunengo[4], Paola Stagnaro[4], Vasile Tiron[5], Petronel Postolache[3], Maria Teresa Buscaglia[6], and Liliana Mitoseriu[3]

[1] *RAMTECH, Sciences Department, Institute of Interdisciplinary Research, Alexandru Ioan Cuza University of Iasi, Blvd. Carol I, Nr. 11, 700506 Iasi, Romania*
[2] *National Institute of Materials Physics, Str. Atomistilor 405A, 077125 Magurele, Romania*
[3] *Faculty of Physics, Alexandru Ioan Cuza University of Iasi, Blvd. Carol I, Nr. 11, 700506 Iasi, Romania*
[4] *Institute for Macromolecular Studies, Section of Genoa, Italian National Research Council, Via De Marini 6, 16149 Genoa, Italy*
[5] *Research Department, Faculty of Physics, Alexandru Ioan Cuza University of Iasi, Blvd. Carol I, Nr. 11, 700506 Iasi, Romania*
[6] *Institute for Condensed Matter Chemistry and Technologies for Energy, Section of Genoa, Italian National Research Council, Via De Marini 6, 16149 Genoa, Italy*

Received: 17 July 2019
Accepted: 6 December 2019
Published online: 12 December 2019

ABSTRACT

In the present work, a magnetodielectric flexible thick film composite with a quaternary $Ba_{12}Fe_{28}Ti_{15}O_{84}$ ferrite filler ($\leq$ 9 vol%) embedded into PVDF polymer matrix was investigated. The role of filler volume on the macroscopic dielectric, magnetic and ferroelectric properties as well as on the nanoscale magnetic and piezoelectric response was analyzed. The formation of small amounts of polar phases besides the majority α-phase of PVDF was shown by XRD and FTIR combined analysis. The electrical properties are dominated by the polymer response, while magnetic order is derived as sum property from the ferrite ones, having a predominant soft magnetic character with small coercivity of $H_c \sim 60$ Oe and high saturation magnetization of $M_s = 2.6$ emu/g for the highest concentration of 9 vol%. Permittivity and losses slightly increase with ferrite filler addition, and the composite maintains a dielectric character for all the compositions. Local PFM and MFM investigations have shown a combined ferro/piezoelectric character and magnetic order, with magnetoelectric coupling demonstrated by the reorientation of filler particles and modifications of local piezoresponse when applying a static magnetic field.

Address correspondence to E-mail: felicia.gheorghiu@uaic.ro

https://doi.org/10.1007/s10853-019-04279-w

Introduction

Over the years, polymer-based composites have gained a great technological interest and became an active area due to the variety of advanced electronics applications such as piezo-sensors, actuators, memory and gate dielectrics for integrated circuits [1–3] and miniaturized capacitors for telecommunication or energy storage devices [4–7]. For such applications, polymers present the advantages of easy processing at low temperatures, flexibility and high dielectric breakdown field. Among the large variety of polymers, PVDF (polyvinylidene fluoride) and its copolymers are the most interesting as matrix for electronic composites, due to their dielectric, pyro-, piezo- and ferroelectric properties. Permittivity of PVDF, as for other polymers, has values of a few units $\sim$ 12 at room temperature [7–9], and one of the most used methods to increase it for applications is to disperse a high permittivity inorganic powder as filler into the PVDF polymer matrix. However, even adding high permittivity ($\sim 10^3$) fillers leads to a modest increase in dielectric constant which remains quite low (usually around 10), even for high filler concentrations. To date, many publications reported studies on PVDF composites with different fillers s such as ferro/piezoelectrics ($BaTiO_3$, $PbTiO_3$, PMN, PZT) [8–11], ferrites or other magnetic materials [12, 13] or polymer-based nanocomposites filled with carbonaceous species as graphene, carbon nanotubes (CNTs) or metallic nanoparticles, to induce good conductive properties or giant capacitance [14–16].

By combining magnetic ordered materials within a ferroelectric PVDF matrix, the major expected result is a magnetoelectric artificial multiferroic material with properties driven by composition and microstructural characteristics (e.g., size and shape, phase mixing, interfaces) together with flexibility. It is well known that PVDF has five crystalline phases denoted as α, β, γ, δ and ε [17–21]. The α-phase is the most stable at ambient temperature and pressure but in the same time is nonpolar due to the antiparallel arrangement of dipole moments. The δ-phase is a polar parallel version of the α-phase, but the two chains in the unit cell are arranged in such a way that the net dipole moment is not zero [18]. The β-phase of the PVDF polymer presents the highest dipole moments that are aligned in the same direction, perpendicular to the macromolecular chain, resulting in a high spontaneous polarization. The γ-phase is polar, but its polarization is very low, and consequently, the ferroelectric properties are very difficult to be experimentally determined. Consequently, in order to exploit the ferroelectric properties, the β-phase appears to be the most desirable phase for the applications aforesaid. The formation of the β-phase can be induced by the processing parameters and filler addition in composites.

Due to its superior characteristics already mentioned, PVDF has been chosen as matrix to host a quite new quaternary ferrite with formula $Ba_{12}Fe_{28}Ti_{15}O_{84}$ (BFT in the following). The phase $Ba_{12}Fe_{28}Ti_{15}O_{84}$ was first reported in 1991 by Grey et al. [22], with a monoclinic $C2/m$ structure symmetry. In a previous paper [23], it was reported the preparation of $Ba_{12}Fe_{28}Ti_{15}O_8$ powders and dense ceramics and some preliminary magnetic characteristics (e.g., ferrimagnetic behavior at room temperature with a saturation magnetization of $\sim$ 12.5 emu/g, coercivity of $\sim$ 20 Oe and Curie temperature of $\sim$ 420 K) have been reported. The $Ba_{12}Fe_{28}Ti_{15}O_{84}$ ceramic shows a real part of permittivity by the order of $\sim$ 25–50 at frequency of 10^9 Hz and much higher values (10^5–10^6) in the low frequencies range that were attributed to extrinsic effects (e.g., semiconductor character and Maxwell–Wagner phenomena). Its crystal structure is described as formed by two blocks (perovskite and spinel building blocks) that are linked by an intermediate layer containing a mixture of titanium and iron ions. Due to its intergrowth type of structure, BFT may exhibit both ferroelectric and magnetic properties as well as a magnetoelectric coupling. However, due to the high dielectric losses and strong extrinsic Maxwell–Wagner phenomena, macroscopic ferroelectricity has not been unequivocally confirmed. It is expected by embedding BFT particles into PVDF matrix to obtain a flexible multiferroic composite with reduced extrinsic contributions to dielectric properties and lower dielectric losses.

Experimental details

Composite thick films with formula $(1-x)$PVDF–(x)BFT (x = 0 vol% ÷ 9 vol%) were prepared by dispersing into the polymeric matrix (PVDF) different volume fractions of BFT powders with homogeneous grain size in the range of (0.3 ÷ 1) μm (Fig. 1) prepared by solid state synthesis, as described in Ref. [23].

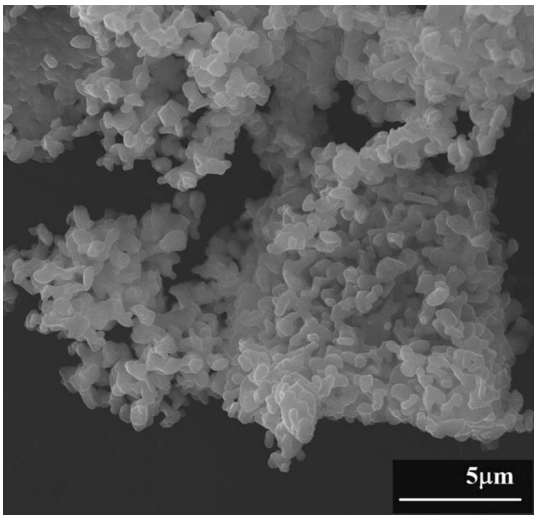

Figure 1 SEM images of the $Ba_{12}Fe_{28}Ti_{15}O_{84}$ powder.

Polyvinylidene fluoride (PVDF, Mw = 175.000, pellets form, supplied by Sigma-Aldrich) was employed as the polymer matrix, using dimethyl formamide (DMF) of 99.5% purity (Merck) as solvent. Firstly, a film of neat PVDF was prepared for reference purpose. The PVDF pellets were dissolved in DMF by magnetically stirring at 65 °C for 2 h to obtain a homogeneous and transparent solution with a mass ratio of 20/80. This solution was poured into a Petri dish and placed in an oven to dry at 165 °C for 4 h. After the complete evaporation of the solvent, a flexible and transparent pure PVDF film was obtained. Afterward, the PVDF–BFT flexible composites were prepared by solution-sonication method (Fig. 2).

The BFT powder was previously functionalized with hydrogen peroxide at 100 °C for 1 h until complete reduction of liquid phase. Surface hydroxylation of the BFT particles is expected to improve their dispersion into the polymeric matrix [18, 24, 25]. This process is expected to favor the β-crystalline phase formation by creating hydrogen bridges with the fluoride groups in the PVDF polymeric chains [25]. The composite films result by dispersing the desired amount of BFT powder in the dissolved PVDF, in concentrations within the range of 0.1–9 vol%. The functionalized BFT particles were placed in DMF and sonicated for 4 h (Fig. 1). Afterward, the PVDF pellets were added to the solvent-particles suspension and mechanically stirred for 2 h at 65 °C (to avoid the agglomeration of the particles due to the magnetization). The obtained mixture was poured into a Petri dish and crystallized at 165 °C for 4 h. Flexible BFT–PVDF membranes with high mechanical strength were obtained after the complete evaporation of the solvent. The optical transparency decreases as the concentration of the filler material increases; the highest concentration leads to an opaque composite, but still flexible (Fig. 2).

The phase composition of the obtained composites was checked with a Shimadzu LabX 6000 diffractometer (CuKα radiation, λ = 0.15406 nm) with scan step increments of 2°/min between $2\theta \in$ (20–80)°. Spectroscopic characterization (FTIR analysis) was performed with a PerkinElmer Spectrum Two™ FTIR spectrometer operating in the attenuated total reflectance (ATR) mode and recording absorbance spectra in the 4000–400 cm^{-1} wave number range. The microstructural features of the cryo-fractured cross sections (fracture performed in liquid nitrogen ambient) of the composites were examined by backscattered-electron (BSE) scanning electron

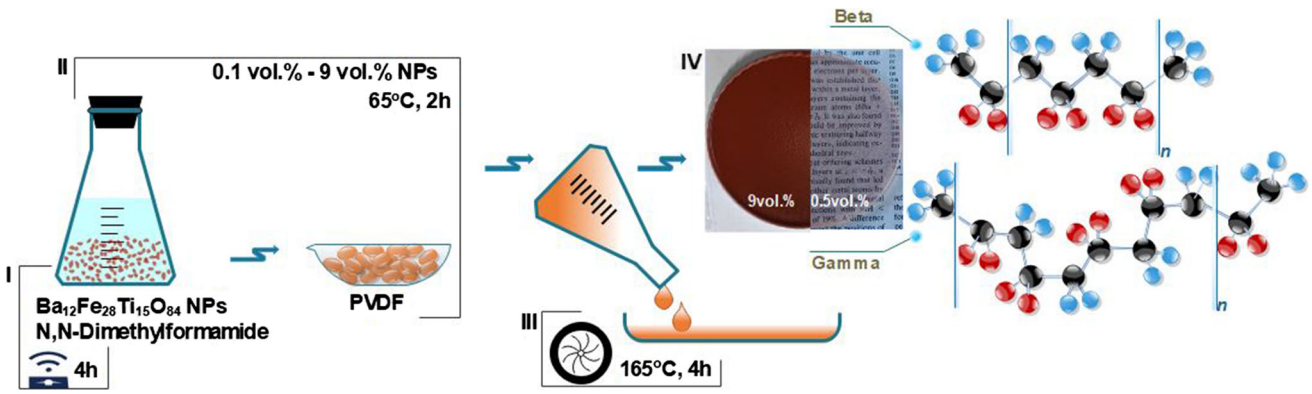

Figure 2 The flowchart preparation of the PVDF–BFT composites.

microscopy (SEM) using a Hitachi S-3400 N II microscope type. For obtaining clear BSE-SEM images, a few nm of gold thin film was deposited by rf-sputtering magnetron system type Q150T S/E/ES on the cross-sectional surface in order to avoid the electrostatic charging. The composites films were shaped in disk form (with diameter of ~ 20 mm and thickness of ~ 0.2 mm) and painted both sides with silver paste electrode. The impedance spectroscopy measurements were carried out using an impedance bridge type Agilent E4980A Precision LCR Meter in the frequency range of $20 \div 2 \times 10^6$ Hz and at different temperatures between 25 and 150 °C. The ferroelectric *P–E* hysteresis loops were recorded at room temperature on electrode samples immersed in transformer oil bath by a Sawyer–Tower modified circuit fed by a high-voltage sine wave (frequency 10 Hz) by using a TREK amplifier. The magnetic *M–H* loops were measured at room temperature with a Vibrating Sample Magnetometer MicroMagTM VSM model 3900 (Princeton Measurements Co.).

Piezoelectric and magnetic force microscopy (PFM & MFM) was employed to investigate the local electromechanical (piezoelectric) and magnetic properties of the PVDF–ferrite composite films using a multi-mode AFM setup (NT-MDT SolvePro). In this work, all the PFM measurements were taken during one imaging session using the same cantilever (CSG10 from NT-MDT, with platinum conductive coating, nominal spring constant of 0.2 N/m and free resonant frequency of 35.9 kHz) and the same laser position in order to allow for quantitative comparison between the investigated samples. PFM images (surface topography, magnitude and phase) were obtained in contact mode at a vertical deflection set point of 2 nm, drive voltage of 1 V and scan rate of 0.5 Hz. The local piezoelectric coefficient (d_{33}) values were estimated from the piezoresponse curves which represent the dependence of the piezoresponse (magnitude signal) versus the applied bias voltage. For each PVDF–ferrite composite sample, the average piezoelectric coefficient d_{33} value was calculated by averaging piezoresponse measurements performed on a matrix (10×10 points) placed on different random areas with surface area of 3×3 μm^2.

For MFM measurements, a NSG01/Co cantilever (with Co magnetic coating, free resonant frequency 374.5 kHz and nominal spring constant 8.1 N/m) was used in non-contact AC magnetic force mode. Microscope controlling, acquisition, processing and analysis of the recorded data were done using *Nova* software from NT-MDT.

Results and discussion

Structural and microstructural characterization

Figure 3 displays the XRD patterns of PVDF, BFT (identified with JCPDS file no. 04-010-4440) and of the $(1-x)$PVDF–(x)BFT composite thick films. The diffraction pattern of neat PVDF film is characterized by the small peaks observed at 2θ of 17.86°, 18.5°, 20.08°, 26.8°, 33.2°, 36.1° and 38.7°. The reflections characteristic to the α-crystalline phase of PVDF are centered at 2θ of 17.7° (100), 18.3° (020), 20.0° (110), 26.6° (021), 33.2° (130), 35.9° (200) and 38.8° (002), while the main peaks corresponding to the γ-phase are located at 2θ of 18.5°(020), 19.2° (002), 20.04°(110) and 39.0°(211) [20, 21]. Thus, the peaks observed for the present composites at 18.5°, 20.08° and 38.7° could be ascribed to the presence of both α- and γ-phases. When BFT particles are incorporated into the PVDF matrix, the diffraction patterns of the composite show as expected the peaks of both parent systems, in a ratio corresponding to the nominal composition.

In order to better identify the α- and γ-phases of PVDF, the thick films were further examined using FTIR analysis.

The corresponding FTIR spectra are shown in Fig. 4. In comparison with database from the literature [18, 20, 21], the collected data show slightly different values, up to ± 5 cm^{-1}. The α-crystalline phase is identified through the peaks around 409, 530, 612, 762, 795, 854, 974, 1147, 1209, 1382 and 1432 cm^{-1}. A peak corresponding exclusively to γ-phase is centered at about 426 cm^{-1}, while two small peaks at 510 and 842 cm^{-1} are ascribable to both the electroactive β- and γ-phases. Taking into account the combined XRD and FTIR experimental evidences, it may be proposed that neat PVDF and composite films are mainly characterized by the α-crystalline phase with small amounts of γ-phase, which is the polar phase with the lowest dipole moment among the PVDF polymorphs. However, the lack of some other characteristic peaks of γ-phase in the recorded IR spectra (namely at 811, 833 and 1234 cm^{-1}) [21] let open the possibility of existence of small amounts of

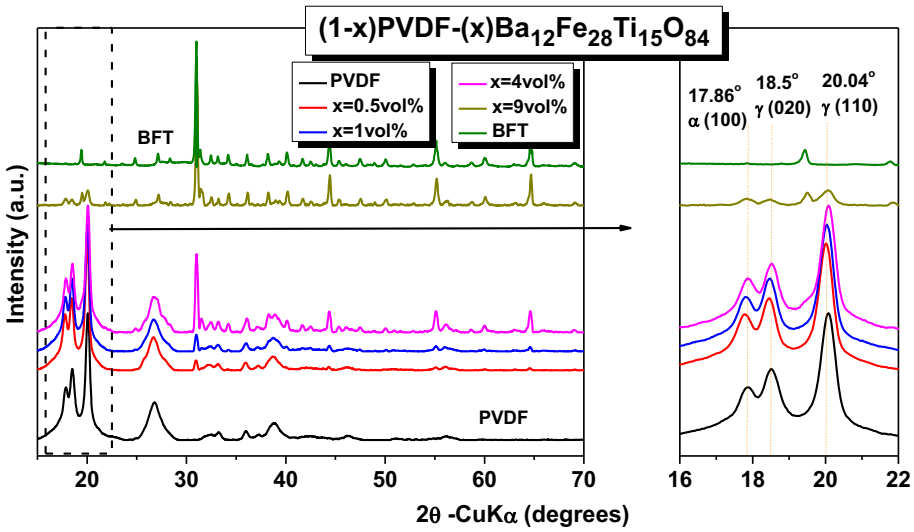

Figure 3 XRD patterns of the $(1 - x)$PVDF–$(x)Ba_{12}Fe_{28}Ti_{15}O_{84}$ composites (BFT diffraction data were indexed with JCPDS file no. 04-010-4440).

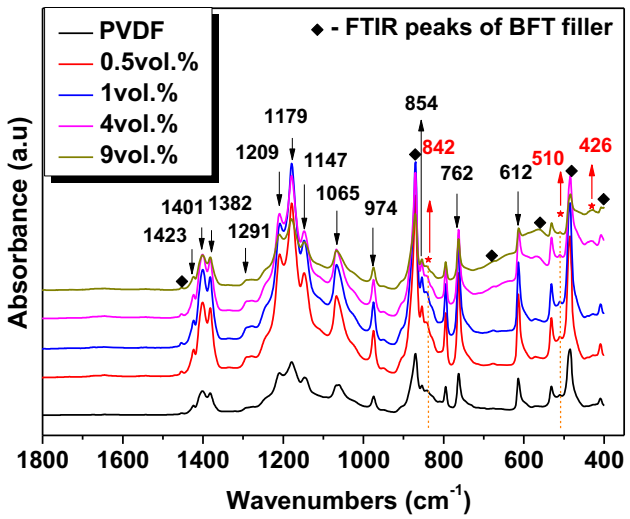

Figure 4 Absorbance FTIR spectra for the $(1 - x)$PVDF–$(x)Ba_{12}Fe_{28}Ti_{15}O_{84}$ composites.

polar β-phase in the composite. The fraction of γ-phase in the composites can be determined using the following formula [26–28]:

$$F(\gamma) = A_\gamma/[(K_\gamma/K_\alpha)A_\alpha + A_\gamma], \quad (1)$$

where A_α and A_γ are the baseline-corrected absorbance at 763 and 512 cm^{-1}, and K_α and K_γ are the absorption coefficient for α- and γ-phases. The values of K_α and K_γ were reported as being equal with 6.1×10^4 cm^2 mol^{-1} and 2.4×10^4 cm^2 mol^{-1}, respectively. The results of the variation in γ-phase with increasing in filler concentration obtained from the FTIR analysis are listed in Table 1. It can be observed that with increasing in the particles concentration the fraction of γ-phase increases.

Table 1 Fraction of γ-phase obtained from FTIR analysis for $(1 - x)$PVDF–$(x)Ba_{12}Fe_{28}Ti_{15}O_{84}$ composites with different concentration of ferrite particles

Samples	$F(\gamma)$
$x = 0$	0.54
$x = 0.5$ vol%	0.62
$x = 1$ vol%	0.64
$x = 4$ vol%	0.69
$x = 9$ vol%	0.72

Figure 5 shows the BSE images of cryo-fractured cross section of the selected $(1 - x)$PVDF–$xBa_{12}Fe_{28}Ti_{15}O_{84}$ thick film composites with $x = 0$, 0.5 and 4 vol% concentrations. The BFT particles are quite homogeneously distributed into the PVDF polymer matrix, which has a wavy aspect (Fig. 5a). In addition, a few aggregates of fine particles and a small degree of porosity can be also noticed in some regions.

Magnetic properties

Figure 6 shows the room-temperature magnetic hysteresis loops for $(1 - x)$PVDF–$(x)Ba_{12}Fe_{28}Ti_{15}O_{84}$ thick film composites. Since PVDF has no magnetic order, the magnetization in these composites is produced by the filler particles as a *sum property*. Therefore, magnetization increases when increasing the BFT particles addition, as expected (Inset of Fig. 6). All the M–H cycles are characterized by a very low coercivity, of $\sim$ 60 Oe, with small remnant and saturation magnetizations: For the highest concentration, $x = 9$ vol%, $M_r = 0.62$ emu/g and $M_s = 2.6$ emu/g, respectively. $Ba_{12}Fe_{28}Ti_{15}O_{84}$ exhibits a soft magnetic behavior ($H_c = 40$ Oe) [23, 29]. Magnetic M–H loops show

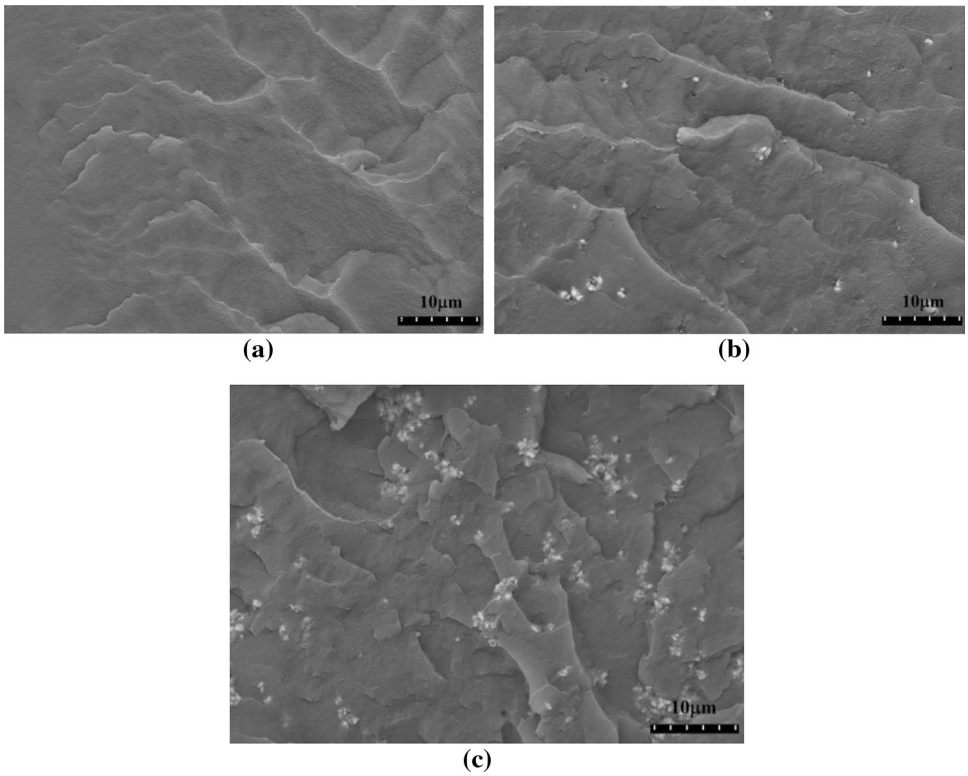

Figure 5 The backscattered-electron images of cryo-fractured cross section of $(1 - x)$PVDF–$(x)Ba_{12}Fe_{28}Ti_{15}O_{84}$ composites for: $x = 0$ (**a**); $x = 0.5$ vol% (**b**) and $x = 4$ vol% (**c**).

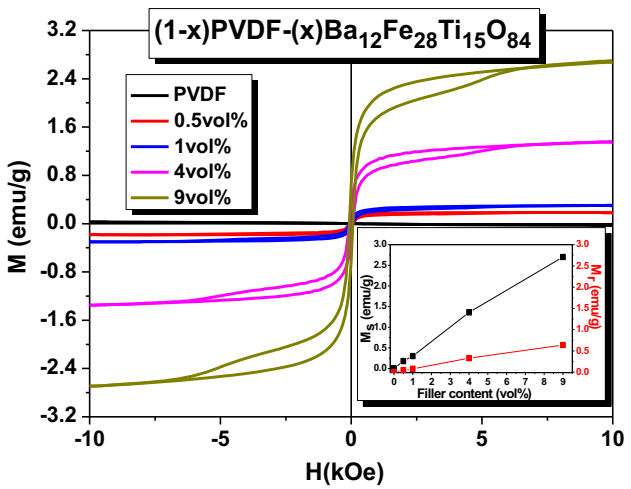

Figure 6 Magnetic hysteresis loops at room temperature for $(1 - x)$PVDF–$(x)Ba_{12}Fe_{28}Ti_{15}O_{84}$ composites. Inset: saturation and remnant magnetizations versus ferrite content.

interesting shapes ("wasp-waisted" saturated loops) originated from the magnetic behavior of BFT filler [23].

The occurrence of such types of loops is due to the presence of two magnetic phases with contrasting coercivities, *i.e.*, a soft and a hard one, as it was reported in previous papers [23, 29]. The hard component is most probably due to very small amounts (below the XRD detection limits of present composites) of a secondary phase like barium hexaferrite ($BaFe_{10.7}TiO_{19}$) existing in the filler particles, as it was reported in a previous paper [23]. (Additional phase was identified by BS-SEM, EDS analyses and thermomagnetic data.) In the literature, it was reported for barium hexaferrite the presence of a hard ferromagnetic behavior at room temperature [21, 30], with a high remnant and saturation magnetization ($M_r \approx 40$ Am^2 kg^{-1} and $M_s \approx 70$ Am^2 kg^{-1}), that can significantly affect the magnetic properties of the composites. In conclusion, the present composites show magnetic order with predominant soft character (very low coercivity), as derived from the filler particles, and they may accomplish the requirements as magnetodielectric materials if dielectric character is predominant.

Dielectric properties

Pure PVDF presents two main dielectric relaxation processes: One at lower temperatures labeled as β in the literature related to the glass transition (assigned to cooperative segmental motions within the main chains of the amorphous regions of the material) and one which appears at temperatures above 80 °C and is associated with molecular motions within the crystalline fraction of the material, denominated as α-

relaxation [31]. Besides these, additional relaxation mechanism due to inhomogeneity might be present in composites.

Figure 7 shows the room-temperature real part of permittivity and conductivity versus frequency dependences of $(1-x)$PVDF–$(x)Ba_{12}Fe_{28}Ti_{15}O_{84}$ composites. The permittivity presents a regular small increase when increasing the amount of BFT inclusions in comparison with values corresponding to pure PVDF: At 100 Hz, permittivity increases from $\varepsilon \sim 8$ for pure PVDF to about ~ 12 for 9 vol% PVDF–BFT composite thick films. It should be mentioned that the small increase in permittivity, in comparison with the literature reports on similar polymer systems doped with ferrite particles [26, 27], is due to the small employed filler concentration which was used in order to not alter the flexibility of these composites. For all the composites, the real part of permittivity reduces when frequency increases from 10^2 to 10^6 Hz. The tangent loss (not shown here) decreases from values about 0.06 for PVDF and 0.11 for $x = 9\%$ at 100 Hz down to minimum values below 0.02 for all the compositions in the frequency range of (10^3–10^5) Hz. A further increase in tangent losses takes place for all the compositions at higher frequencies, when tanδ reaches ~ 0.2 at 1 MHz. The increased real part of permittivity at low frequency range ($< 10^3$ Hz) indicates some extrinsic electrical polarization phenomena contributions, *e.g.*, electrode polarization and Maxwell–Wagner–Sillars (MWS) interfacial polarization [23, 32, 33]. The interfacial polarization gives contribution due to the change from the internal interfaces, while electrode polarization arises from changes between the dielectric material and electrodes [33]. The MWS polarization effect increases when the filler concentration is higher, resulting in an enhancement of permittivity. This polarization arises from the volume

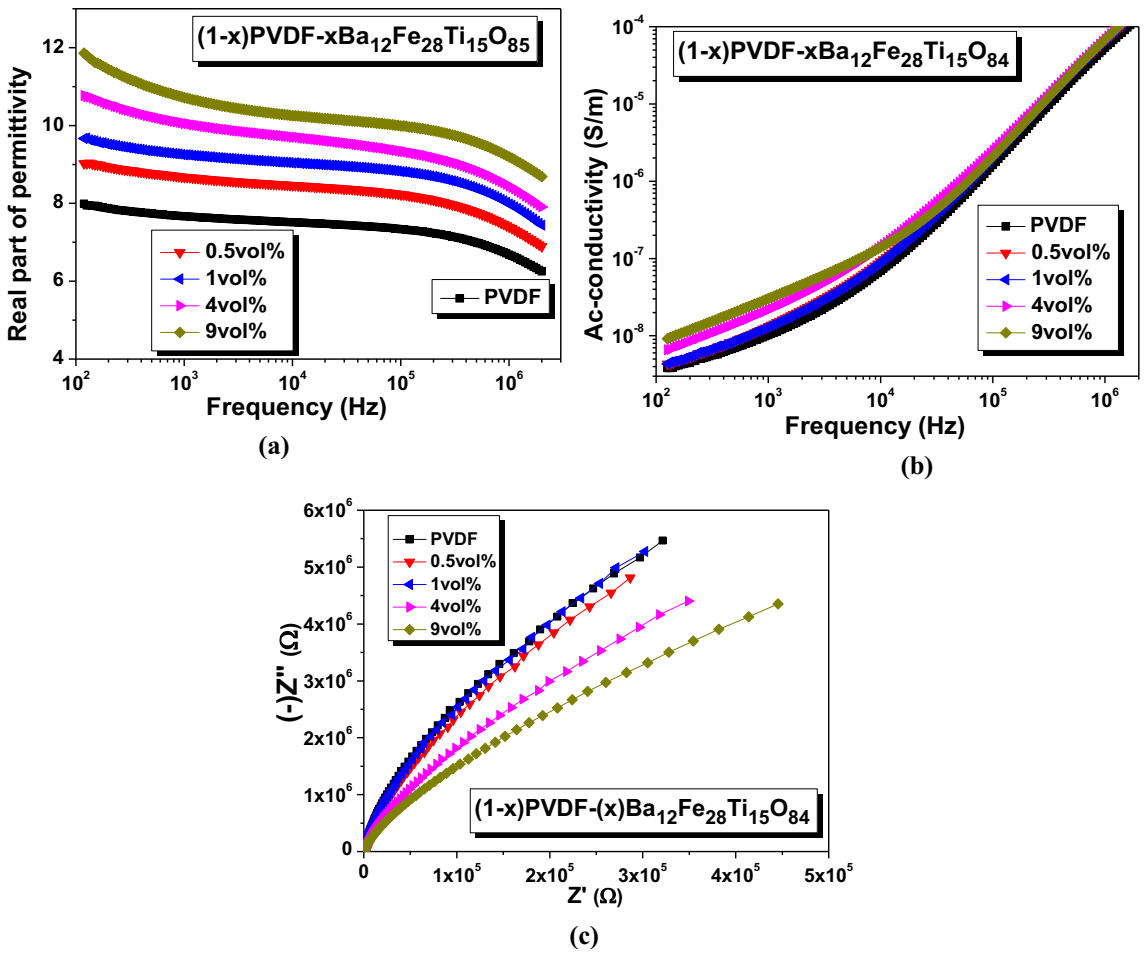

Figure 7 Room-temperature dielectric properties of $(1-x)$PVDF–$(x)Ba_{12}Fe_{28}Ti_{15}O_{84}$ composites: frequency dependences of the real part of permittivity (**a**) and AC conductivity (**b**); complex impedance plot (**c**).

uncompensated charges due to the local electrical inhomogeneity (local variations of permittivity and conductivity) in heterogeneous materials, as composites, while in semicrystalline polymers, and is due to variations of electrical properties between its amorphous and crystalline phases. This polarization mechanism leads to high values of the real part of permittivity accompanied by the highest losses in low frequency range. Above 10^3 Hz, this contribution vanishes and it is expected to obtain the intrinsic dielectric response of thick film composites. However, at frequency of 1 MHz, drops of permittivities together with a strong increase in losses are found and these effects might be attributed to another relaxation mechanism activated in this frequency range.

Figure 7b shows the frequency dependences of the electrical conductivity for the PVDF–BFT composites. It can be observed that the introduction of BFT particles results in a slightly increase in conductivity of about three times in $x = 9$ vol% with respect to ones in pure PVDF. The general trend of increasing conductivity with frequency rise in pure PVDF does not seem to change with the filler addition. For all the composites, the conductivity presents strong frequency dependence and exhibits values in the range of 10^{-4}–10^{-9} S/m, which are typical for semiconductors [23]. Figure 7c shows the complex impedance data measured at room temperature for $(1-x)$PVDF–$(x)Ba_{12}Fe_{28}Ti_{15}O_{84}$ composites. The complex impedance plot, i.e., the $Z''(Z')$ dependence shown in Fig. 7c, reveals an apparent single component, which demonstrates a good dielectric and conductivity homogeneity within the sample.

Figure 8a–f shows the evolution with frequency of the imaginary part of permittivity and of the imaginary part of dielectric modulus at few selected temperatures, for three selected composites with $x = 0$, 0.5 and 4 vol% content of BFT. The obtained results for the imaginary part of permittivity (Fig. 8a–c) are similar for the all composites and show that ε'' regularly increases with the temperature increase. From Fig. 8d–f, it can be observed that the amplitude of M'' decreases when increasing the ferrite concentration. Because a relaxation peak was obtained in the measured domain of frequencies, it might be concluded that at least one relaxation-like mechanism contributes to the dielectric response in the investigated frequency range. This mechanism is thermally activated, and the frequency corresponding to the M'' maximum shifts toward higher frequencies when increasing temperature and the observed phenomena are similar, irrespective of composition. Only at high temperatures of 130 °C and 150 °C, a second relaxation-like mechanism is visible in M'' by the appearance of a shoulder in the high-frequency side well distinguished in composites ($x = 0.5$ vol% and 4 vol%).

A similar behavior has been reported for $BaTiO_3$–PVDF composites [34], and it was attributed to MWS interfacial polarization. Apparently, pure PVDF does not show this component, although the M'' peak at 150 °C is slightly non-symmetric (Fig. 8d), and therefore, the MWS mechanism seems to be at the origin of this relaxation.

For a better understanding of this relaxation process, activation energies were calculated by using the Arrhenius analysis, from the frequencies and temperature dependences of the imaginary part of dielectric modulus (Fig. 9). All the present $(1-x)$PVDF–$(x)Ba_{12}Fe_{28}Ti_{15}O_{84}$ composites show similar values for the activation energy of about $\sim$ 0.68 eV, irrespective of filler addition, and the same value was also found in pure PVDF. This might give the idea that the presence of filler does not change this relaxation, which should originate from the PVDF matrix. Similar activation energies in the range of 0.4–0.7 eV were usually associated with the crystalline α-relaxation of polymers related to the macromolecular chains motions in the crystalline regions [34, 35].

According to the literature [36], there are three relaxation modes in PVDF: (i) α_a-relaxation that appears for temperatures between −48 and −10 °C and for frequencies between 10^{-1} and 10^6 Hz and is associated with the glass transition of the PVDF matrix; (ii) α_c-relaxation that is associated with the molecular motions in PVDF crystalline region and occurs between 0 and 150 °C (between $10^{-1} \div 10^6$ Hz); and (iii) relaxation that is associated with the interfacial polarization that can be observed in semicrystalline polymers. Therefore, it appears more likely that the relaxations from Fig. 8d–f, for the temperature up to 130 °C, are related mainly to the pure PVDF chains motions (α_c-relaxation) and for the highest temperature appears a second relaxation associated with the MWS interfacial polarization [34, 36].

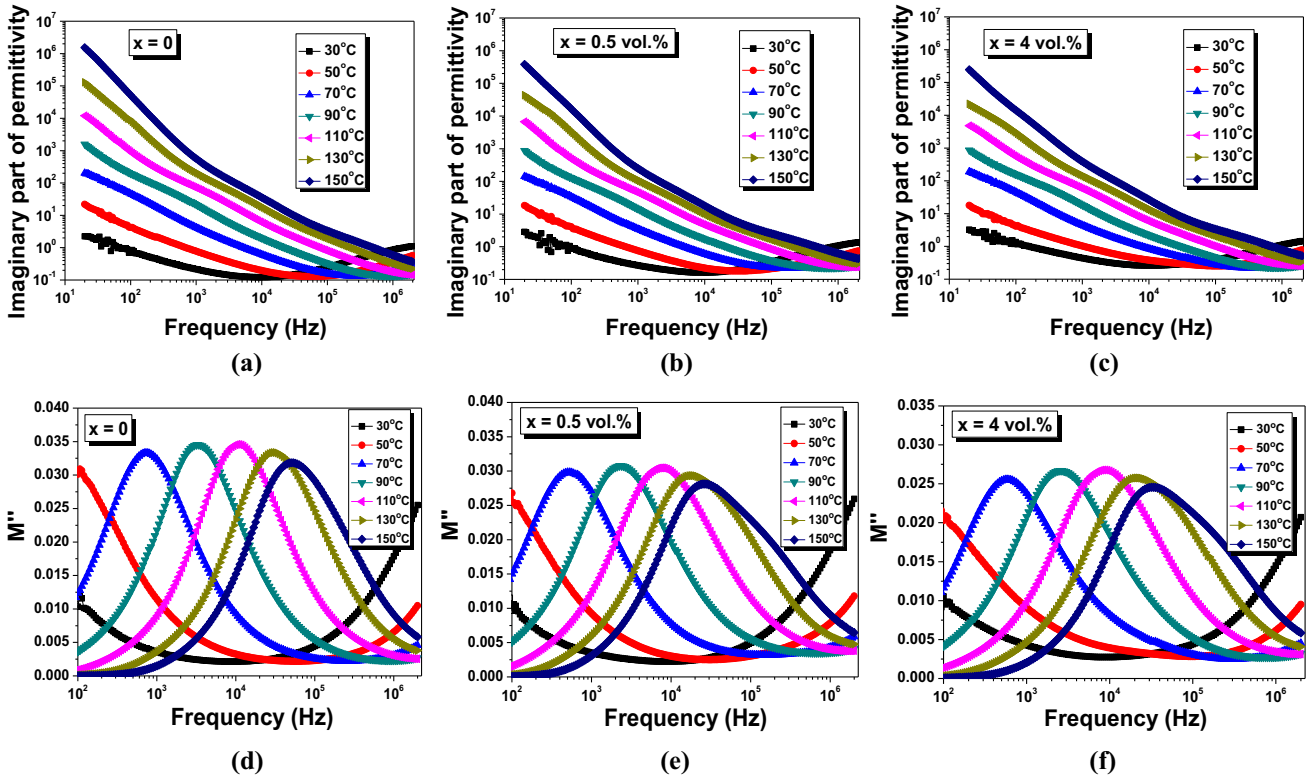

Figure 8 Frequency dependences of the real part of permittivity and imaginary part of dielectric modulus at various temperatures for $(1 - x)$PVDF–$(x)Ba_{12}Fe_{28}Ti_{15}O_{84}$ composites.

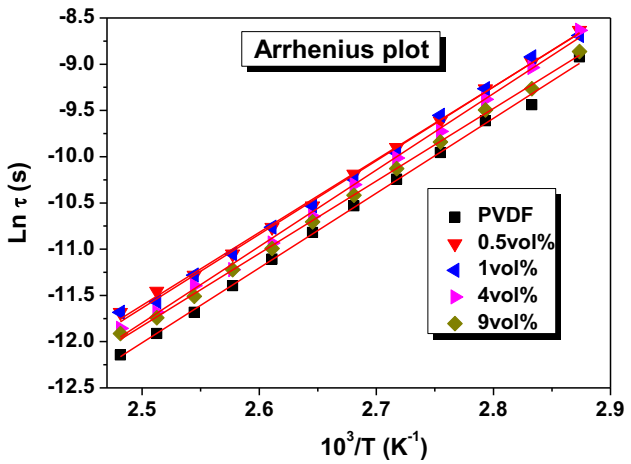

Figure 9 Arrhenius plot determined from the maximum of the imaginary part of dielectric modulus.

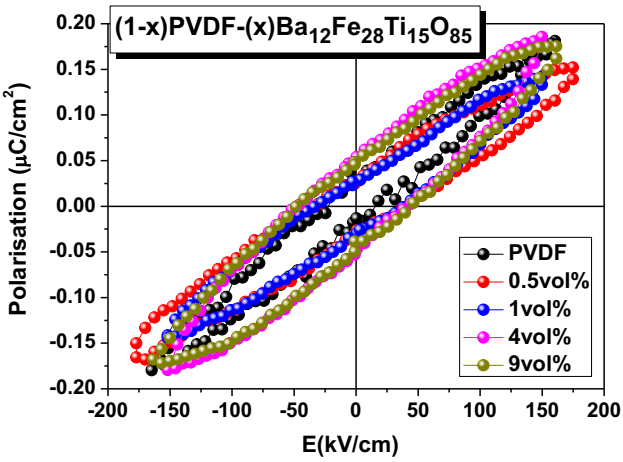

Figure 10 The *P–E* hysteresis loops measured at room temperature for PVDF–BFT composites.

Ferroelectric properties

The room-temperature *P–E* hysteresis loop for $(1 - x)$PVDF–$(x)Ba_{12}Fe_{28}Ti_{15}O_{84}$, measured at the same applied field, is comparatively presented in Fig. 10. All the samples show well reproducible high field responses, due to their low losses. For all the filler additions, these loops are still non-saturated at 150 kV/cm and the application of higher fields leads to the dielectric breakdown of composites with high BFT content (9 vol%).

The polarization maximum increases monotonically and reaches value of 0.175 μC/cm^2 for the composite with 9 vol% BFT. As previously

mentioned in Ref. [23], BFT has a semiconductor behavior, so that the sample with the highest filler amount also shows the highest conductivity. As expected, the slope of the hysteresis loops systematically increases when increasing the volume fraction of BFT particles, this slope being related to the dynamic permittivity which also increases when increasing the filling factor. Similar effects were reported for different types of ferroelectric-polymer composites [37]. At the maximum available field, the remnant polarization P_r shows a systematical increase, from 0.02 μC/cm^2 for 0.5% BFT to 0.05 μC/cm^2, while the maximum of polarization for the composite with the highest volume fraction of BFT increases from 0.15 to 0.18 μC/cm^2. The results indicate that the BFT particles contribute to the effective polarization of the composites.

PFM and MFM characterization

In order to check the ferroelectric/piezoelectric and magnetic domain patterns for the $(1-x)$PVDF–$(x)Ba_{12}Fe_{28}Ti_{15}O_{84}$ composite films, the PFM and MFM techniques were used. Figure 11 shows the PFM images that corresponds to the topography, magnitude and phase responses for PVDF–ferrite composites with x = 0, 4 and 9 vol% content of BFT particles. For the pure PVDF sample, it can be observed a slight texture pattern in both magnitude (piezoresponse signal) and phase images that may be related to the fact that PVDF polymer contains a small amount of polar γ-phase besides the majoritary α-polymorph. This statement is also supported by its average piezoelectric constant d_{33} (4 pmV^{-1}), which is much lower than values reported in the literature (20–28 pmV^{-1}) [38]. In contrast with the pure PVDF polymer, the magnitude and phase images of PVDF–ferrite composite films show a variety of contrasts implying widespread of local piezoresponse and allow identifying domain structures with different orientations of polarization. The PFM images show that the polarization of the polymer–ferrite composites films is changed when electric field is applied, which demonstrates the small ferroelectric/piezoelectric character of the measured samples.

AFM morphology measurements evidenced an increase in root-mean-square roughness (R_{rms}) with the increasing percentage of BFT. For polymer composites with of 0, 4 vol% and 9 vol% of BFT, R_{rms} values of 3 nm, 7.5 nm and 9.6 nm were estimated from topography images. No particular morphologies allowing to exactly detect the placement of regions with polar α- or γ-phase as reported in Ref. [39] for PVDF–CNT composites are found here. The average piezoelectric coefficients d_{33} also increase with the increasing of particles concentration, from 4 pmV^{-1} (x = 0) to 10 pmV^{-1} (x = 4 vol%).

An indirect proof of the magnetoelectric (ME) effect was obtained by using PFM mode under application of a magnetic field (with B = 1500 G) on the films with x = 4 vol% (Fig. 12). It is clear that the presence of the magnetic field influences the orientation of the BFT particles (bright contrast in Fig. 12a) in comparison with the PFM images before (Fig. 11b) and after the magnetic field application (Fig. 12b).

In polymer composite containing both ferroelectric and magnetostrictive phase, when an external magnetic field is applied, the composite system becomes strained. Because of the coupling between the magnetic and ferroelectric domains, the strain induces stress that in turn generates additional charges on the ferroelectric domain. Therefore, a magnetic field applied to the polymer composite will produce a deformation via magnetostriction, which will be coupled to the piezoelectric phase resulting in an induced polarization. In this study, when an external magnetic field is applied to the PVDF composite samples, a clearly reorientation of the magnetic particles occurs. The feature sizes in topography image are comparable to those in magnitude and phase images, and the boundaries of uniformly polarized regions (the bright contrast from magnitude image) coincide with topographic features, which indicate an enhanced piezoelectric response around the BFT particles. The applied magnetic field is expected to modify the alignment of the magnetic particles via magnetostriction which induces a strain in the magnetostrictive phase. The induced stress is then transmitted to the ferroelectric PVDF phase, which undergoes a change in its electrical polarization by piezoelectric effect. The change in electrical polarization can also be linked to the phase transformation in the PVDF polymer. This is consistent with the mechanism proposed by Martins et al. [40] which show that the essential factor for the nucleation of the β-phase in the PVDF–ferrite composites is the static electric interaction between the magnetic particles and the CH_2 groups of PVDF having a positive charge density. However, with these experiments it is